

Supporting Information

© Wiley-VCH 2013

69451 Weinheim, Germany

Understanding CO₂ Dynamics in Metal–Organic Frameworks with Open Metal Sites**

Li-Chiang Lin, Jihan Kim, Xueqian Kong, Eric Scott, Thomas M. McDonald, Jeffrey R. Long, Jeffrey A. Reimer, and Berend Smit*

anie_201300446_sm_miscellaneous_information.pdf

Supporting Information

Contents

Section 1: Experimental details.

Section 2: Simulation details.

Section 3: CSA pattern of the hopping motion between the 6 minimum energies configurations.

Section 4: Visualization of CO₂ equilibrium configurations and dynamic trajectories.

Section 1: Experimental details:

I. Sample preparation

General. The ligand $H_4(\text{dobpdc})$ was synthesized as previously reported.^[1] All other reagents were obtained from commercial vendors at reagent grade purity or higher and used without further purification. A modified synthesis of $Mg_2(\text{dobpdc})$, described below, was utilized.

$Mg_2(\text{dobpdc})$. Into a 35-mL Pyrex cell, $H_4\text{dobpdc}$ (120 mg, 0.438 mmol), $MgBr_2 \cdot 6H_2O$ (300 mg, 0.925 mmol), and 15 mL of solvent (1:1 DMF:EtOH) were loaded and sealed with a PTFE cap. The mixture was irradiated in a microwave reactor (CEM Discover) for 30 min at 120 °C. After 30 min, the solution was cooled and the resulting solid was collected via filtration and soaked in hot DMF overnight at 80 °C. The product was collected via filtration, rinsed with CH_2Cl_2 , and transferred to a Schlenk flask. Under flowing N_2 , the product was heated at 420 °C for 65 min and then cooled to room temperature in vacuo. The flask was transferred to a dinitrogen filled glovebox. Activation of the product was confirmed via agreement of the N_2 adsorption isotherm of the material at 77 K with that of the previously reported material.¹

II. NMR measurement

Before NMR experiments, the sample were evacuated under vacuum of $\sim 10^{-7}$ torr at 430 K for 12 hours. ^{13}C labeled CO_2 (99%, purchased from Sigma-Aldrich) was then cryo-pumped and sealed into the glass NMR tubes with the evacuated MOF samples under liquid nitrogen temperature.

^{13}C NMR spectra were collected at 7.05 Tesla with a ^{13}C frequency of 75.5 MHz. Measurements of the sample were performed with a home-made non-resonant probe and a Tecmag LapNMR spectrometer, using a 90° pulse of 15 μs . The sample temperature was maintained with an Oxford Instruments SpectrostatNMR continuous flow cryostat. The amount of CO_2 was calibrated at 298 K to the signal intensity of a ^{13}C labeled glycine sample with known quantity. NMR spectra were obtained via appropriately phase-cycled averages following spin echoes with 40 μs echo time. The total acquisition time for each spectrum varied in order to achieve a reasonable signal-to-noise ratio.

Section 2: Simulation details:

I. Molecular simulation description

In this study, the canonical Monte Carlo simulations (NVT simulation) were carried out to probe the free energy landscape of CO₂ molecule (i.e., obtain possible CO₂ configurations) in Mg-MOF-74 for further analyses at various temperatures. Each simulation has total 10⁷ Monte Carlo steps including translation, rotation, and regrow moves. Configurations were recorded with the interval of every 10² Monte Carlo steps, resulting in total 10⁵ different configurations from each simulation. In addition, the MD simulation was used to illustrate the dynamic trajectories with sufficiently small time step (i.e., 0.5 fs) in the following SI section 4. In the MD simulations, the canonical ensemble was adopted with the Nose-Hoover thermostat.

In these simulations, we assumed the framework to be rigid and used the DFT fully relaxed structure for our calculations.^[2] The simulation box contains multiple unit cells in order to have the length at least twice the cut-off radius, which was set to be 12.8 Å, in each perpendicular directions. Both dispersive and electrostatic energies were included to model the guest-framework and the guest-guest interactions. The Lennard-Jones potential was adopted to describe the dispersion interaction, in which we used the universal force field (UFF)^[3] for the framework atoms and TraPPE model^[4] for the CO₂ molecule. Finally, the partial charges of the Mg-MOF-74 framework atoms were computed using the REPEAT algorithm⁵ while the partial charges of the Mg₂(dobpdc) were obtained from the values published in the previous study directly.^[2] The classification of the atom-types in the framework and the parameters of both dispersive and electrostatic interactions are summarized in the following Section 2-II and Section 2-III.

II. Definition of atom types in the framework

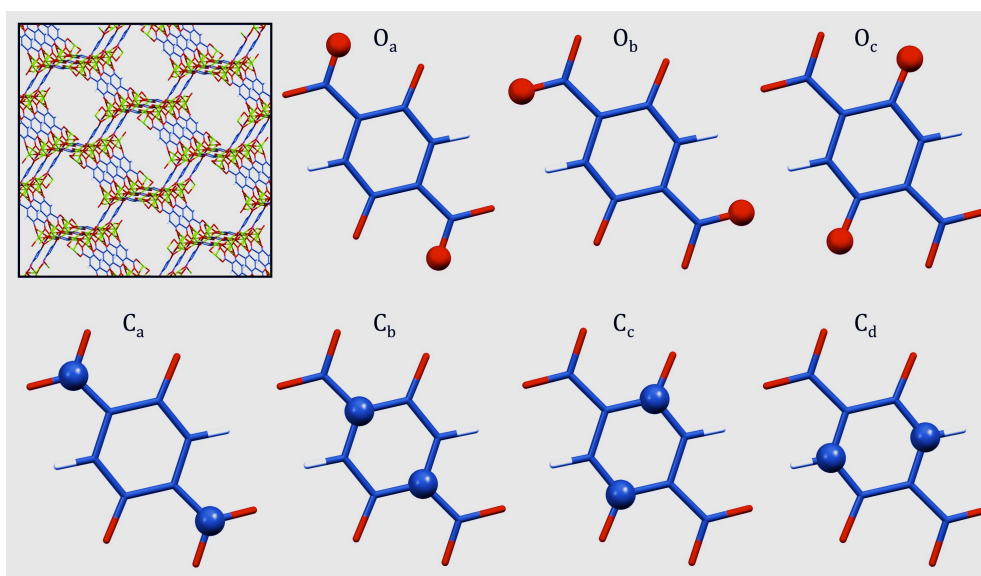


Figure SI 1: Image of Mg-MOF-74 structure (top left) where it is seen that all metal types (Mg, green color) are equivalent, and BDC linker atom types considered in this work. There are total 9 atoms types including hydrogen.

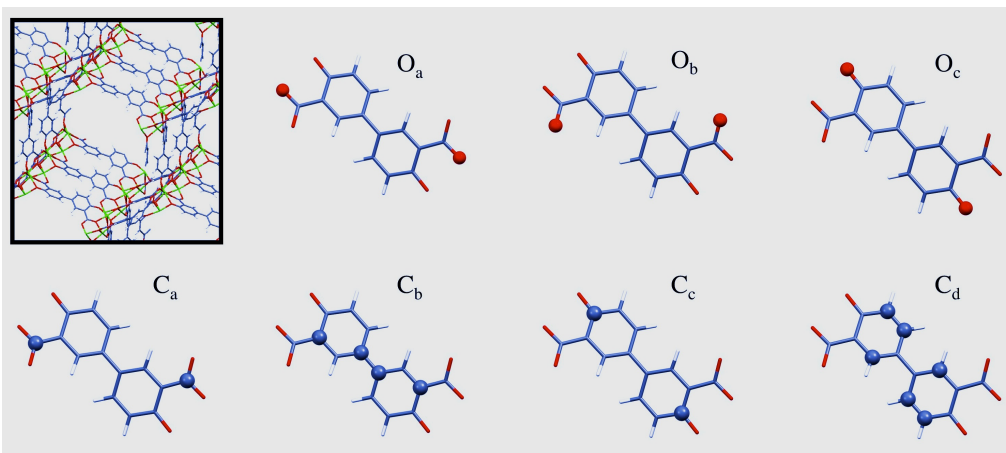


Figure SI 2: Image of $\text{Mg}_2(\text{dobpdc})$ (left), an expanded version of the Mg-MOF-74 structure, where it is shown that all Mg types (green color) are equivalent. Same naming scheme is used as for the Mg-MOF-74 structure shown in Figure SI 1.

III. Force field parameters and atomic charges used in the molecular simulations

Potential parameters for the Lennard-Jones potential model, and atomic partial charges are summarized in the tables below. Table SI 1 gives the Lennard-Jones parameters for framework atoms and guest molecules. The parameters of framework atoms were taken from the universal force field (UFF),^[3] and the parameters of the guest molecules were adopted from TraPPE model.^[4] The Lorentz-Berthelot mixing rules were used for the interaction between any two different atom types. Table SI 2-3 give the atomic charges of the framework atoms. The partial charges of the Mg-MOF-74 framework atoms were computed using the REPEAT algorithm^[5] while the partial charges of the $\text{Mg}_2(\text{dobpdc})$ were obtained from the values published in the previous study directly.^[2] Table SI 4 gives the charges of guest molecules obtained from TraPPE model.^[4]

Table SI 1: Lennard-Jones parameters for framework atoms and guest molecules.

Atom	Lennard-Jones parameters	
	Epsilon (K)	Sigma (Å)
Mg	55.85	2.69
O _a	30.19	3.12
O _b	30.19	3.12
O _c	30.19	3.12
C _a	52.84	3.43
C _b	52.84	3.43
C _c	52.84	3.43
C _d	52.84	3.43
H	22.14	2.57
O(CO ₂)	79.00	3.05
C(CO ₂)	27.00	2.80

Table SI 2: Charges for framework (Mg-MOF-74) atoms.

Atom	Charges (e)
Mg	1.4902
O _a	-0.8149
O _b	-0.6949
O _c	-0.8840
C _a	0.7904
C _b	-0.2774
C _c	0.4362
C _d	-0.2284
H	0.1828

Table SI 3: Charges for framework (Mg₂(dobpdc)) atoms.

Atom	Charges (e)
Mg	1.55271
O _a	-0.77003
O _b	-0.7136
O _c	-0.83773
C _a	0.47603
C _b	-0.15132
C _c	0.20064
C _d	-0.14577
H	0.27731

Table SI 4: Charges for guest molecules.

Atom	Charges (e)
O(CO ₂)	-0.350
C(CO ₂)	0.700

IV. Chemical shift anisotropy (CSA) pattern calculation

The ¹³C chemical shift for an axially symmetric molecule such as CO₂ in this study is obtained by the following equation:

$$\omega(\theta) = -\omega_{ref} - \frac{1}{2}\Delta(3\cos^2\theta - 1)$$

We use the values of ω_{ref} and Δ equal to -133 ppm and 224 ppm, respectively, for the CO₂ molecule in this study. θ is the angle between the O=C=O molecule and the applied magnetic field direction. Within the sampling time scale of the NMR experiments (i.e., a few microseconds), it is reasonable to make the assumption that the CO₂ molecules would visit all the equilibrium configurations obtained from the NVT simulations. It is important to note that, for the localized fluctuation motion, only a subset of all obtained equilibrium configurations is selected and then used in the CSA pattern calculations. The selection criterion is based on the distance between open metal sites and the closest O(CO₂) atom of each CO₂ configuration, which is set

to be smaller than 3 Angstrom. For a given direction of applied magnetic field, the ^{13}C chemical shift is averaged of these configurations. The final computed CSA pattern is then given by powder average (i.e., approached by applying 50000 uniformly random oriented magnetic fields in this work).

Section 3: CSA pattern of the hopping motion between the 6 minimum energies configurations

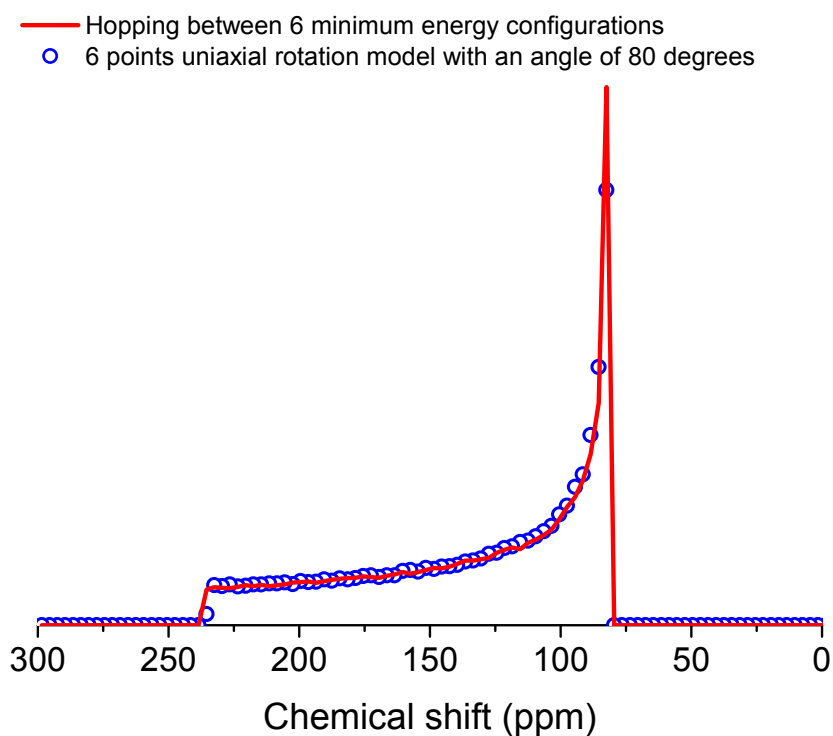


Figure SI 3: Comparison of the computed CSA patterns between the hopping motion between the 6 minimum energies configurations with equal probabilities (solid red line) and the 6 points uniaxial rotation model (equal probabilities) with a fixed angle of 80 degrees (open blue circles). From the comparison, it clearly indicates that the hopping motion between these minimum energies configurations has an equivalent rotational angle of 80 degrees.

Section 4: Visualization of CO₂ equilibrium configurations and dynamic trajectories

Figure SI 4 and Figure SI 5 provide orthographic views along the Z-direction of the possible CO₂ configurations obtained from the NVT simulation at different temperatures, 50 K and 250 K, in Mg-MOF-74 structure. We observe, from these configurations, two types of motion of the CO₂ molecules: (1) fluctuation of the CO₂ molecule near the minimum energy configuration (illustrated in Figure 1b of the manuscript) and (2) hops between different metal sites (Figure 1c of the manuscript). Furthermore, the locations of C(CO₂) are projected on the X-Y, X-Z, and Y-Z plane as closed dots, which are shown in Figure SI 6, Figure SI 7, and Figure SI 8, respectively. The definition of the coordinate system is given in Figure 1c of the manuscript. In these plots, only the configurations with distance between the selected open metal sites (i.e., the most lower corner Mg sites in a channel as shown in Figure 1c of the manuscript) and the closest O(CO₂) smaller than 3 Angstrom are used. The coordinates of each plot is chosen as the locations of C(CO₂) with respect to the closest open metal site (i.e., as the origin point). From the comparison between the configurations at 50 K and 250 K, it indicates that the movement of CO₂ along the Z-direction is enhanced at higher temperature. As a result, the equivalent rotational angle decreases upon increasing temperature as mentioned in the manuscript.

In addition, MD trajectories of a single CO₂ molecule in Mg-MOF-74 structure at 200 K with the time period of 5 ns is illustrated in Figure SI 9 (perspective view) and Figure SI 10 (orthographic view along the Z-direction), which clearly show that the CO₂ molecule is not simply adsorbed on a open metal site but moves around between different metal sites. For further analyses, the channel profile of the structure is parameterized as a function of both the angular angle and the position along the channel direction, which is schematically shown in Figure SI 11. Figure SI 12 shows the angular angle of the position of C(CO₂) as a function of time (ns), which indicates that the CO₂ performs the non-localized (hopping) motions. Within the time scale of a few nano-seconds, the CO₂ hops between different metal sites in the X-Y plane frequently. It is important to note that there are 6 different open metal sites along the X-Y plane within a unit cell, resulting in the interval of 60 degrees between two adjacent metal sites. Figure SI 13 illustrate the position of C(CO₂) along the Z-direction as a function of time (ns), which further shows that the CO₂ molecule also hops along the Z-direction. The unit cell of the structure along the Z-direction (i.e., the crystallographic c-axis) has the length of ~7 Angstroms.

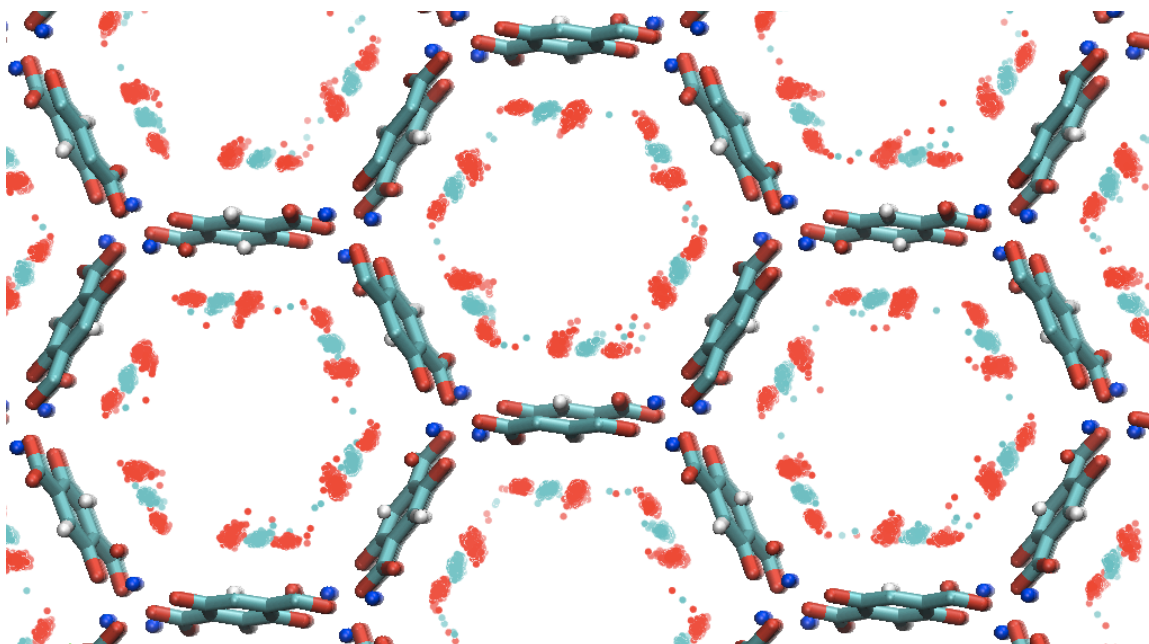


Figure SI 4: Orthographic view along the Z-direction of the CO₂ configurations obtained from the NVT simulation at 50 K in Mg-MOF-74 structure. The CO₂ molecule is represented as closed dots with C (cyan) and O (red). The framework is represented as spheres and bonds with Mg (blue), C (cyan), O (red), and H (white).

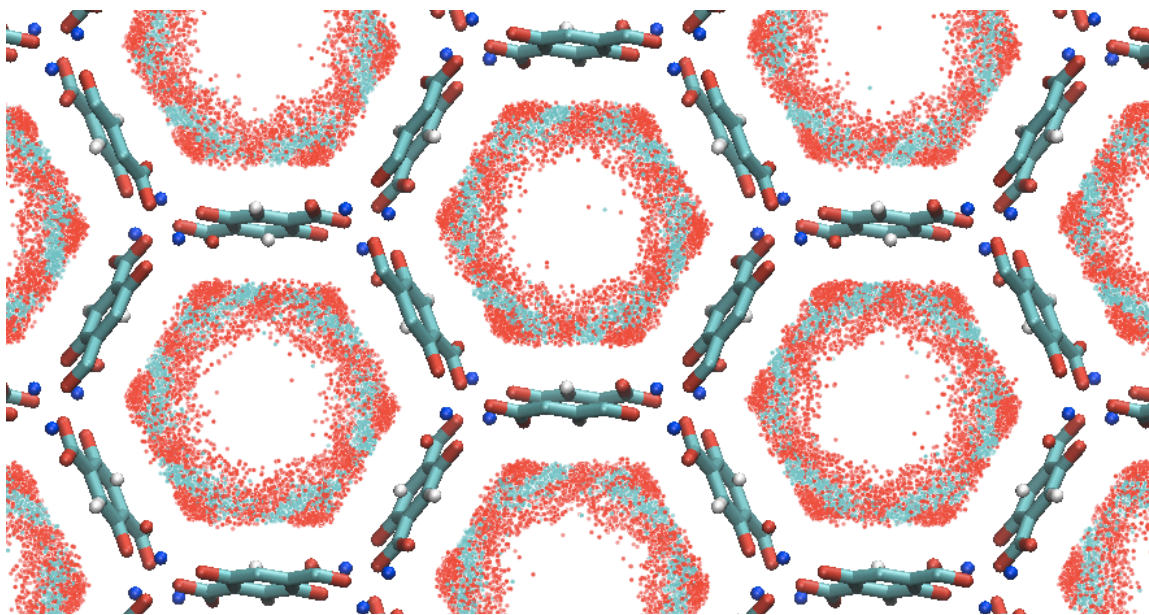


Figure SI 5: Orthographic view along the Z-direction of the CO₂ configurations obtained from the NVT simulation at 250 K in Mg-MOF-74 structure. The CO₂ molecule is represented as closed dots with C (cyan) and O (red). The framework is represented as spheres and bonds with Mg (blue), C (cyan), O (red), and H (white).

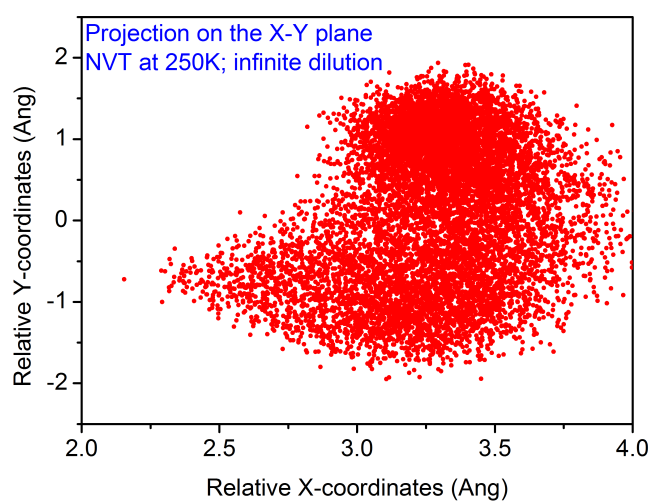
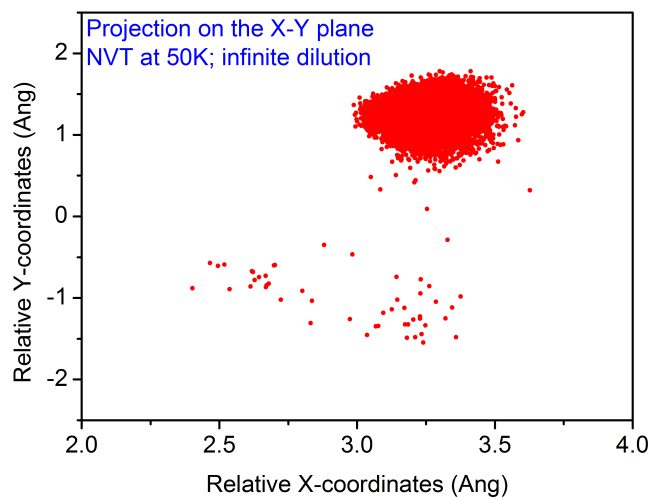


Figure SI 6: Projection of the location of C(CO₂) as closed dots on the X-Y plane at different temperatures, 50 K (upper) and 250 K (lower).

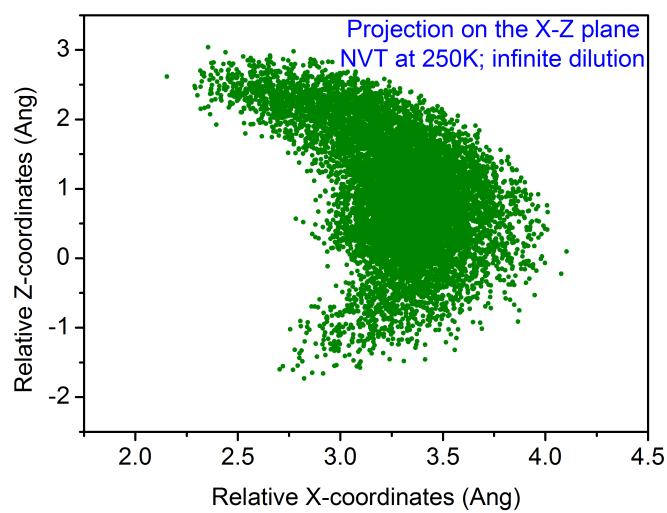
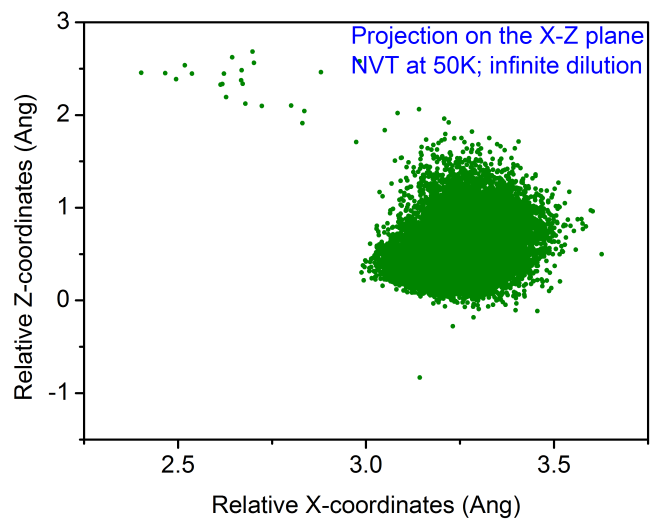


Figure SI 7: Projection of the location of C(CO₂) as closed dots on the X-Z plane at different temperatures, 50 K (upper) and 250 K (lower).

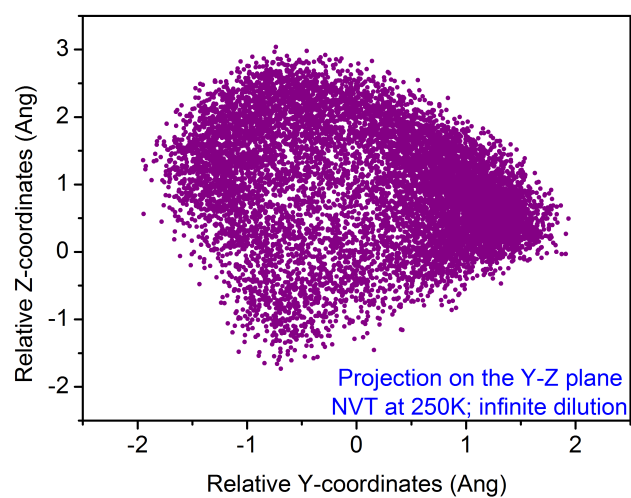
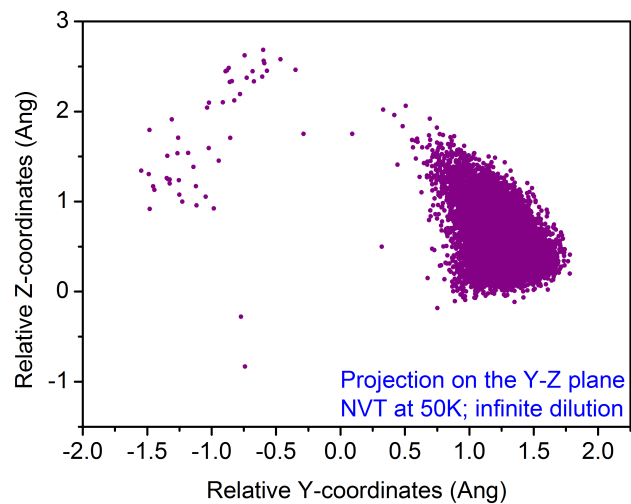


Figure SI 8: Projection of the location of C(CO₂) as closed dots on the Y-Z plane at different temperatures, 50 K (upper) and 250 K (lower).

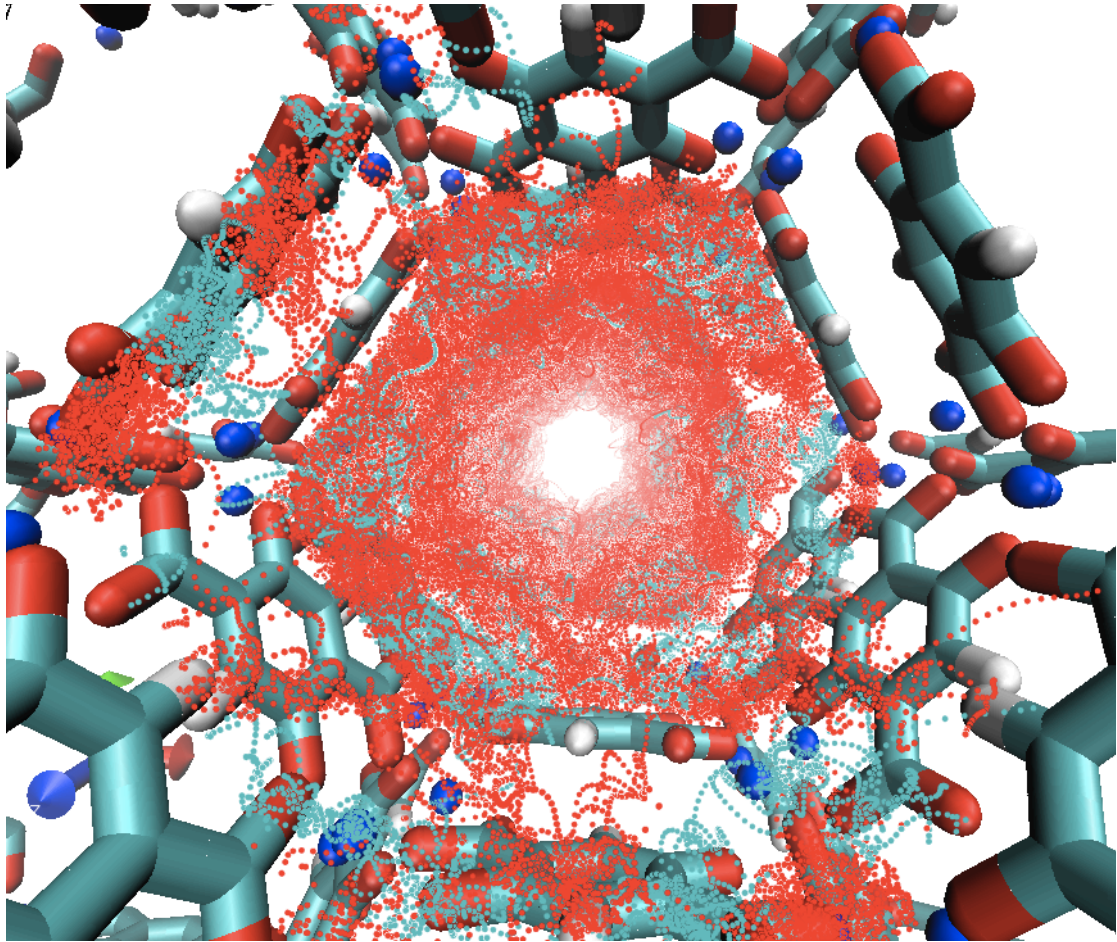


Figure SI 9: Perspective view of the MD trajectories of a single CO₂ at 200 K with the time period of 5 ns in Mg-MOF-74 structure. The CO₂ molecule is represented as closed dots with C (cyan) and O (red). The framework is represented as spheres and bonds with Mg (blue), C (cyan), O (red), and H (white).

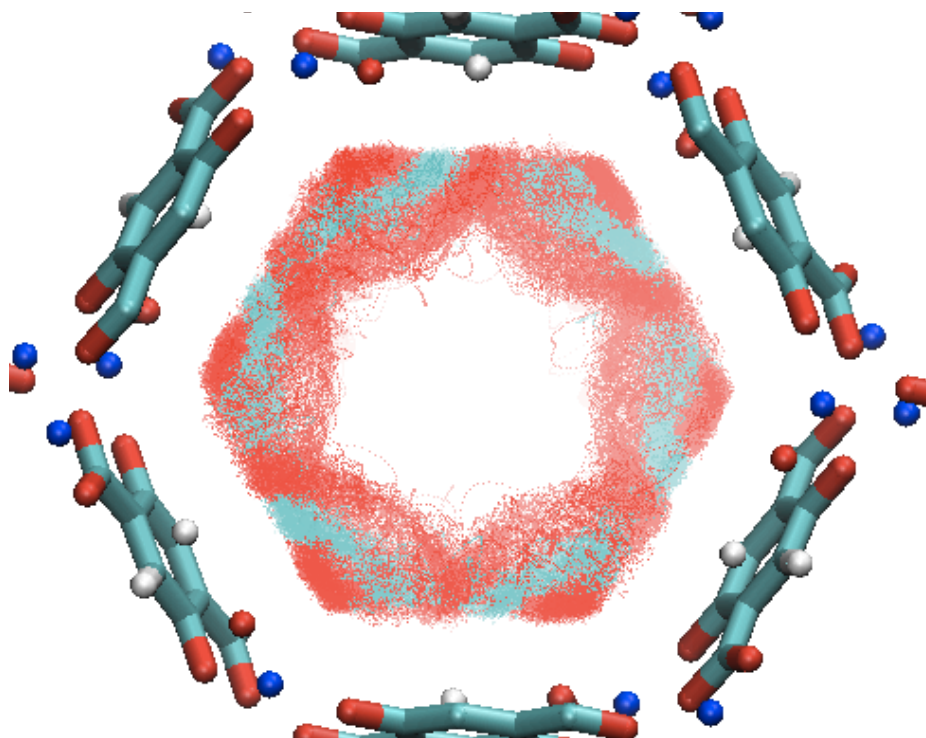


Figure SI 10: Orthographic view along the Z-direction of the MD trajectories of a single CO₂ at 200 K with the time period of 5 ns in Mg-MOF-74 structure. The CO₂ molecule is represented as closed dots with C (cyan) and O (red). The framework is represented as spheres and bonds with Mg (blue), C (cyan), O (red), and H (white).

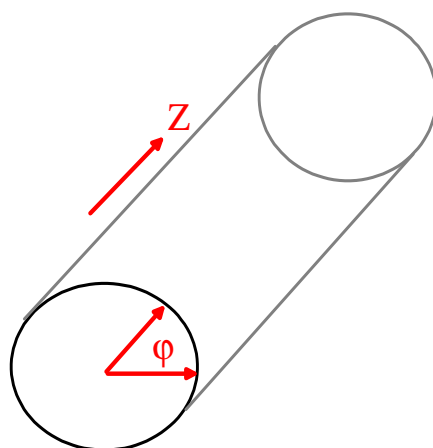


Figure SI 11: Schematic plot of the channel profile as a function of two variables: angular angle of the channel opening and the position along the channel direction (i.e., Z-direction).

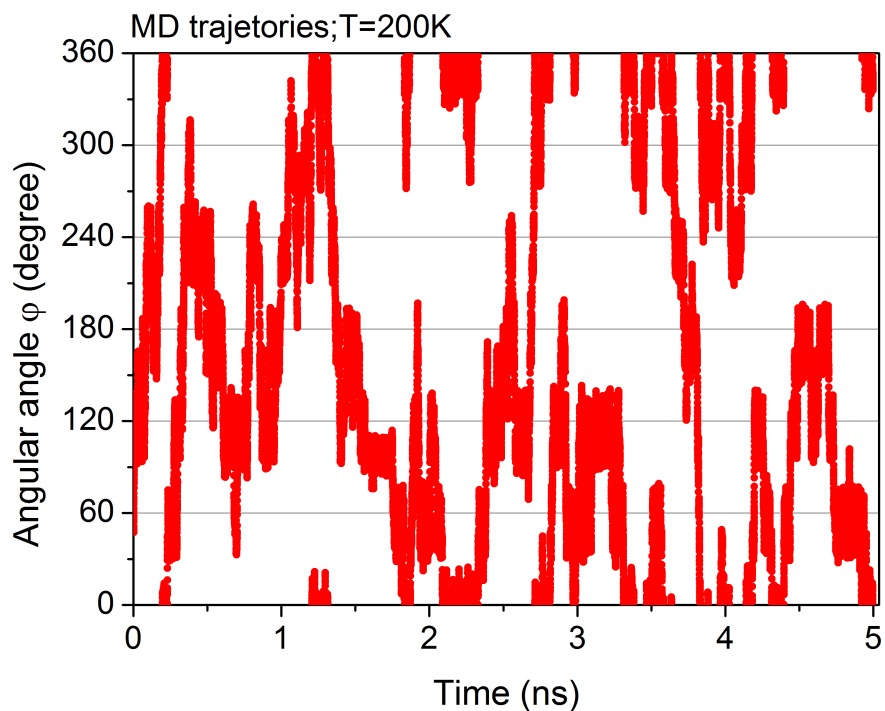


Figure SI 12: MD trajectories of a single CO₂ at 200 K. The angular angle ϕ (degree) of the position of C(CO₂) as a function of time (ns).

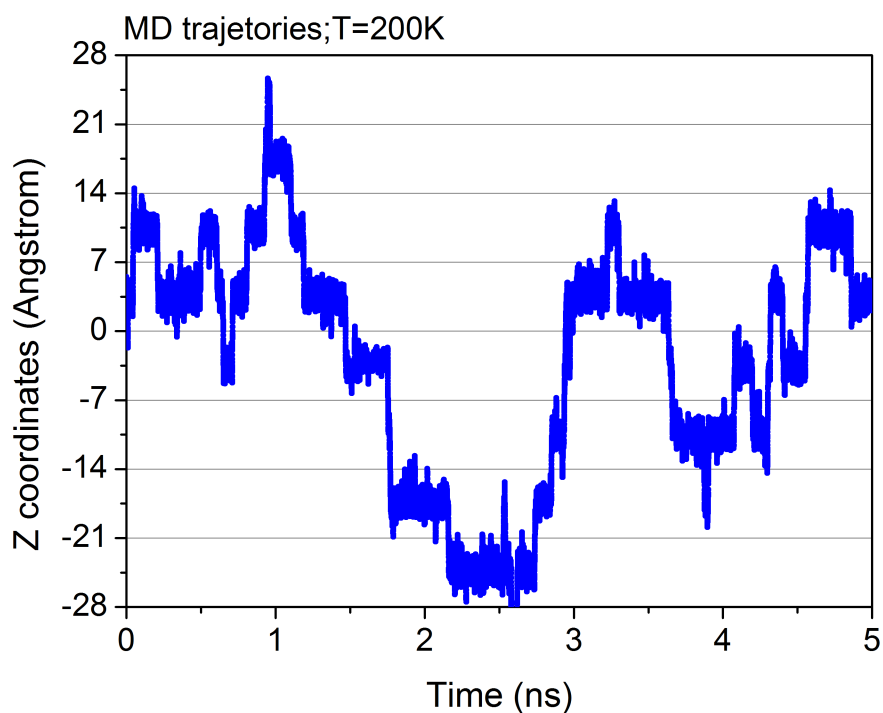


Figure SI 13: MD trajectories of a single CO₂ at 200 K. The position of C(CO₂) along the Z-direction as a function of time (ns).

Reference:

- [1] T. M. McDonald, W. R. Lee, J. A. Mason, B. M. Wiers, C. S. Hong, J. R. Long, *J. Am. Chem. Soc.* **2012**, 134, 7056-7065.
- [2] A. L. Dzubak, L.-C. Lin, J. Kim, J. A. Swisher, R. Poloni, S. N. Maximoff, B. Smit, L. Gagliardi, *Nat. Chem.* **2012**, 4, 810-816.
- [3] A. K. Rappe, C. J. Casewit, K. S. Colwell, W. A. Goddard, W. M. Skiff, *J. Am. Chem. Soc.* **1992**, 114, 10024-10039.
- [4] J. J. Potoff, J. I. Siepmann, *AIChE J.* **2001**, 47, 1676-1682.
- [5] C. Campaña, B. Mussard, T. K. Woo, *J. Chem. Theory Comput.* **2009**, 5, 2866-2878.